Phys Chem Minerals (2006) 33: 98–105
DOI 10.1007/s00269-006-0058-1

ORIGINAL PAPER

Siew Wei Goh · Alan N. Buckley · Robert N. Lamb
William M. Skinner · Allan Pring · Haipeng Wang
Liang-Jen Fan · Ling-Yun Jang · Lee-Jene Lai
Yaw-wen Yang

Sulfur electronic environments in α-NiS and β-NiS: examination of the relationship between coordination number and core electron binding energies

Received: 29 August 2005 / Accepted: 25 November 2005 / Published online: 2 February 2006

Abstract X-ray photoelectron spectra have been obtained under the same experimental conditions for synthetic α-NiS and natural β-NiS in order to establish any difference in S electronic environment, and to test the proposition that S core electron binding energies increase measurably with coordination number when the same metal is in different sulfide structures or lattice sites. The Ni and S electronic environments in the two NiS structures have been further probed by near-edge X-ray absorption fine structure (NEXAFS) spectroscopy, and the NEXAFS spectra interpreted by reference to spectra simulated by ab initio calculations. The photoelectron and NEXAFS spectra for freshly prepared surfaces of α-NiS and β-NiS were found to be similar, with only subtle differences in electronic environment evident in the experimental and simulated NEXAFS spectra. The measured and calculated core electron binding energies did not support the previously postulated relationship between S coordination number and electron binding energies.

Keywords Millerite · α-NiS · XPS · NEXAFS

S. W. Goh · A. N. Buckley (✉) · R. N. Lamb
Surface Science and Technology, School of Chemistry,
The University of New South Wales, 2052 Sydney,
NSW, Australia
E-mail: a.buckley@unsw.edu.au
Tel.: +61-2-93854645
Fax: +61-2-96621697

W. M. Skinner
Ian Wark Research Institute, University of South Australia,
5095 Mawson Lakes, SA, Australia

A. Pring · H. Wang
The South Australian Museum, North Terrace,
5000 Adelaide, SA, Australia

L.-J. Fan · L.-Y. Jang · L.-J. Lai · Y. Yang
NSRRC, 30077 Hsinchu, Taiwan

Introduction

In the interpretation of sulfur core electron spectra for 'fully coordinated' (sub-surface) sulfur atoms in metal sulfides, it is often assumed that sulfur core electron binding energies increase significantly with coordination number. Although there is no general relationship between binding energy and stereochemistry, in many situations initial state effects have a greater influence on binding energy shifts than final state effects (Mårtensson and Nilsson 1995), and an additional implicit assumption, supported by experimental observations (e.g., Bagus et al. 1999), of a change in binding energy with a change in coordination number is common. In particular it has been noted that, almost invariably for materials that are at least moderately ionic, the binding energy is larger for cations at the surface than in the bulk, whereas it is smaller for anions (Egelhoff 1987). This behavior has been interpreted as an initial state effect of lower coordination number at the surface. A related line of reasoning is based on the observation of typical relationships between coordination and oxidation state (e.g., Ravel 2004) and between oxidation state and binding energy. Of course such correlations must be interpreted with care, and indeed the very low S $2p_{3/2}$ binding energy (160.6 eV relative to Au $4f_{7/2} = 84.0$ eV) for the 6-coordinate S atoms in PbS (Clifford et al. 1975; Buckley and Woods 1984) shows there is no general relationship between sulfur binding energy and sulfur stereochemistry even in metal sulfides. However, for a particular metal in different sulfide structural environments, the correlation may have some justification. When this assumed correlation between coordination number and core electron binding energy has been extended to incompletely coordinated sulfur in the outermost surface layer of a particular metal sulfide, it has been postulated that the loss of one coordinating cation causes a negative binding energy shift of about 0.8 eV (Schaufuß et al. 1998).

Significantly different binding energies for 4- and 5-coordinate S atoms in pentlandite, $(Ni,Fe)_9S_8$, were first proposed in an attempt to interpret the S 2*p* spectrum for fresh surfaces of that mineral (Legrand et al. 1997). Pentlandite has two distinct S environments, 25% 4-coordinate and 75% 5-coordinate (Rajamani and Prewitt 1973), and these were assigned S $2p_{3/2}$ binding energy values of 161.4 and 162.2 eV, respectively (Legrand et al. 1997). More recently, high resolution S 2p spectra for the monoclinic pyrrhotite Fe_7S_8 and the hexagonal pyrrhotite $Fe_{10}S_{11}$ have been fitted with contributions from 5-coordinate and 6-coordinate S with binding energies near 161.25 and 162.15 eV, respectively (Nesbitt et al. 2001). Nevertheless, it is clear that the sulfur binding energies in Ni sulfides are not determined solely by the sulfur coordination number when a second metal ion is involved. This is illustrated by the 5-coordinate S in β-NiS (millerite) having a S $2p_{3/2}$ binding energy of 161.6–161.7 eV (Buckley and Woods 1991a; Legrand et al. 1998), at least 0.5 eV lower than for the 5-coordinate S in pentlandite.

While it is not in doubt that the 5-coordinate S in pentlandite has a S $2p_{3/2}$ binding energy of 162.2 eV, the assignment of the component near 161.4 eV to 4-coordinate sulfur in pentlandite is contentious in that an alternative explanation is possible (Legrand et al. 1997; Buckley and Woods 1991b). Notwithstanding electron microprobe analyses of the regions investigated by XPS that indicate compositions within the pentlandite range, it is possible for another Ni/Fe sulfide phase to be present near the surface. For example, it is possible that violarite, $FeNi_2S_4$, may be present at freshly exposed surfaces of pentlandite either as a surface oxidation product or as a pre-existing weathering product, and that the S 2*p* binding energy for the 4-coordinate sulfur in violarite (Vaughan and Craig 1985) may be near 161.4 eV (Buckley and Woods 1991b). Pentlandite usually occurs in intimate association with pyrrhotite, but the principal S $2p_{3/2}$ binding energy for the latter is 161.25 eV (Nesbitt et al. 2001).

Assignment of the S 2*p* spectrum for pyrrhotite is less contentious, but not indisputable. The S $2p_{3/2}$ binding energy for troilite (FeS), in which all S atoms are 6-coordinate (Keller-Besrest and Collin 1990), had been reported as 161.2 eV (Thomas et al. 2003) but a more recent value of 161.85 eV is considered correct (Skinner et al. 2004). The latter value is 0.3 eV lower than that deduced from the pyrrhotite S 2*p* spectrum (Nesbitt et al. 2001).

There is some theoretical evidence to indicate that a binding energy/coordination number correlation exists for a particular metal in different nitride lattice environments. An investigation of the effect of a change of coordination number on core energy levels for different ScN structures predicted that both the N 1*s* and Sc 2*s* binding energies would increase with coordination, the N 1*s* binding energy by 0.3 eV for an increase in coordination from 4 to 5 and by a further 0.2 eV for an increase in coordination to 6 (Šimůnek et al. 2005).

To test the general proposition that S core electron binding energies increase with coordination number, it is pertinent to establish whether this relationship is valid for the case of a particular metal in different sulfide environments, preferably Ni and preferably S in coordinations 5 and 6 to facilitate comparison with the analogous pyrrhotite Fe system. These criteria are satisfied by hexagonal α-NiS and rhombohedral β-NiS, in which the S atoms are all either 6-coordinate or 5-coordinate, respectively. In this report, the S core electron binding energies for freshly prepared surfaces of α-NiS and β-NiS have been determined under the same experimental conditions. The Ni and S electronic environments have been further probed, also under the same experimental conditions, by Ni L-edge, S K-edge and S L-edge near-edge X-ray absorption fine structure (NEXAFS) spectroscopy. X-ray absorption was determined in total fluorescence yield (TFY), as well as in total electron yield (TEY), in order to obtain information representative of the bulk and hence to eliminate the influence of any surface reconstruction. The NEXAFS spectra have been interpreted by reference to spectra simulated by ab initio (predominantly FEFF8) calculations.

Experimental and computational details

The β-NiS investigated was a natural specimen of millerite from Western Australia. The hexagonal α-NiS, perhaps more accurately represented as $Ni_{1-\delta}S$, was necessarily a synthetic specimen, as this form of NiS only exists stably at room temperature when quenched from above 379°C (Trahan et al. 1970).

The α-NiS was prepared by heating stoichiometric amounts of Ni metal (1 mm wire, Sigma 99.99%) and S (flakes, Sigma 99.99%) in a sealed evacuated silica tube slowly to 800°C, maintaining the tube at 800°C for 5 h and then quenching it in water. The charge was ground, resealed in a silica tube under vacuum, annealed at 800°C for 7 days, cooled slowly to 500°C, and then quenched in cold water. The powder X-ray diffraction pattern was recorded using a HUBER Imaging Plate Guinier X-ray diffraction camera (670 model) with Co $K_{\alpha 1}$ radiation. The pattern showed the material to be essentially pure α-NiS. The unit cell analysis and refinement were performed using the Le Bail fitting routines in the program package RIETICA (Hunter 1998), and these indicated a hexagonal unit cell with parameters ($a = 0.34422(3)$ nm; $c = 0.53588(3)$ nm; $\alpha = \beta = 90°$, $\gamma = 120°$) very close to the published values (Trahan et al. 1970; McWhan et al. 1972). The α-NiS was examined by transmission electron microscopy to check for evidence of departure from the ideal NiAs subcell structure. The fragments were ground under acetone in an agate mortar and the resultant suspension dispersed on Cu grids coated with holey-carbon support films. The grids were analyzed using a 200 kV Philips CM200 electron microscope fitted with a standard

side-entry goniometer (±60°), objective lens with $C_s = 2.00$ mm and a W filament. The electron diffraction patterns were free from superlattice reflections and diffuse scattering and consistent with α-NiS in space group $P6_3/mmc$.

For spectroscopic analysis, single-piece specimens of approximate size 5×5 mm^2 were mounted with screws on the same metallic specimen holder as soon as possible after the surface of each NiS specimen had been cleaned by abrasion and subsequent washing with propan-2-ol. Spectroscopic analyses were carried out at room temperature, approximately 2 weeks after the α-NiS had been synthesized. Therefore less than 0.5% β-NiS would have been present in the α-NiS specimen when analyzed. Wang et al. (2006) have shown that at ambient temperature, α-NiS transforms relatively slowly into β-NiS, such that 6 months after synthesis, less than 3.5% of the rhombohedral phase is present.

Conventional monochromatized Al K_α XPS measurements were carried out on a VG ESCALAB 220-iXL spectrometer. An analyzer pass energy of 20 eV and an electron take-off angle of 90° were used, the latter to maximize the analysis depth. Included in the binding energies used for calibration was 83.96 eV for Au $4f_{7/2}$ of metallic gold.

S 1s core electron binding energies and S K-edge NEXAFS spectra were determined on BL15B at the NSRRC, Taiwan. The double crystal monochromator of BL15B was equipped with Si(111) crystals providing a resolution of ~0.35 eV at the S K-edge. S 1*s* binding energies were determined at a photon energy of 3.5 keV. Ni and S L-edge NEXAFS spectra were determined on BL24A at the NSRRC using 1,600 and 400 L/mm gratings, respectively, in the SGM. The NEXAFS spectra were determined in TEY (drain current) and TFY modes, the latter by means of a multichannel plate partial yield detector with the negative retard potential of sufficient voltage to allow for the presence of higher order radiation.

Density of states calculations and NEXAFS spectra simulations were carried out using version 8.20 of the FEFF program for both an unscreened and fully screened core hole (Ankudinov et al. 2002). The absolute energies in FEFF8 are based on atomic total energy calculations using the Dirac-Fock-Desclaux atom code (Ankudinov et al. 1998, 2002). Although the accuracy of this approximation is claimed to be a few electron volt at best (for low atomic numbers), the precision is expected to be significantly better. Self-consistent scattering potentials were calculated within a 0.7 nm radius cluster, equivalent to about 100 atoms, around the absorbing S atom with 15% overlap of the muffin tin radii. A Dirac–Fock/Hedin–Lundqvist exchange potential was used. Full multiple scattering calculations were carried out with cluster radii up to 1 nm, equivalent to about 300 atoms, at which size convergence was achieved. The input files for running FEFF8 were generated by the program ATOMS via the graphical interface TkATOMS (Ravel 2001). The crystallographic structure data used in the calculations were those reported by Trahan et al. (1970) for α-NiS, and Grice and Ferguson (1974) for millerite.

Results

Photoelectron spectra

The S 2*p* photoelectron spectra from the abraded surfaces of α-NiS and β-NiS, shown in Fig. 1, were almost identical, and the S $2p_{3/2}$ binding energy for α-NiS was only ~0.05 eV lower than the value (161.7 eV) for β-NiS. The spectra were broadened on the high binding energy side, as both forms of NiS have metallic conductivity at room temperature and asymmetric lineshapes arise from materials with a high density of states at the Fermi level (Doniach and Sunjic 1970; Citrin 1973). Because of this conductivity, specimen charging was not a problem, and an electron flood gun was not required. Therefore the very small but reproducible binding energy difference observed was unaffected by measurement artifacts. The corresponding C 1*s* peaks from adventitious carbon on the abraded surfaces were at the same binding energy. Both the form of the S 2*p* spectrum, and the S $2p_{3/2}$ binding energy, for β-NiS (millerite) are similar to those observed in previous investigations (Buckley and Woods 1991a; Legrand et al. 1998; Nesbitt et al. 2001). The corresponding S 2*p* binding energy difference for fracture surfaces of α-NiS and β-NiS prepared under vacuum was also small (0.1 eV) (Skinner et al. 2005, unpublished data).

The Ni 2*p* spectra for the two Ni sulfides were essentially the same, and both Ni $2p_{3/2}$ binding energies were at 853.1 eV. The photoelectron spectra in the valence and near-valence region (Fig. 2) displayed only minor differences, and confirmed that the Fermi edge for both sulfides was at a binding energy of 0.0 eV. These spectra were similar to those previously reported for NiS

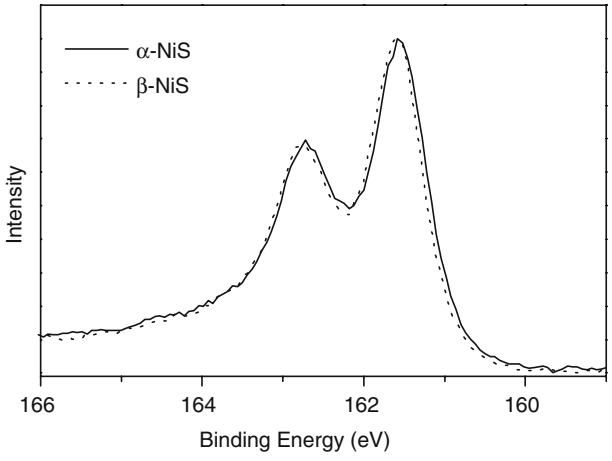

Fig. 1 Normalized S 2*p* photoelectron spectra of α-NiS (*solid line*) and β-NiS (*broken line*)

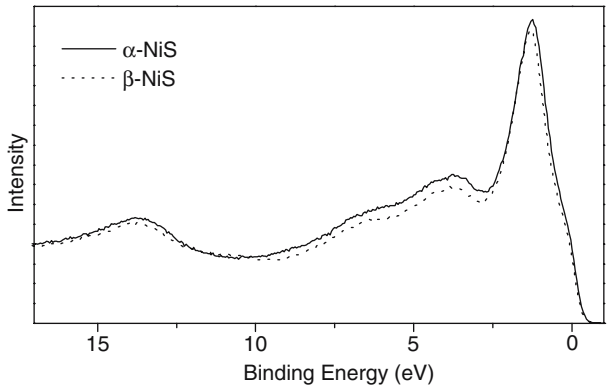

Fig. 2 Photoelectron spectra in the valence and near-valence region for α-NiS (*solid line*) and β-NiS (*broken line*) normalized at 20 eV

(Krishnakumar et al. 2000). The slight intensity difference for the S 3*p* peak near 4 eV relative to the Ni 3*d* peak near 1.5 eV was consistent with (ground-state) densities of states calculated using density functional theory (Raybaud et al. 1997) and FEFF8 (Fig. 3). Other densities of states calculated for α-NiS (Krishnakumar et al. 2000; Zajdel et al. 1999; Usuda and Hamada 2000) and for β-NiS (Krishnakumar et al. 2002) were broadly similar to those obtained using FEFF8. The density of unoccupied states for α-NiS calculated using FEFF8.2 with the Hedin-Lundqvist potential (Kravtsova et al. 2005) was also similar to that obtained in the present work.

Given a S 2*p* binding energy difference of only ~0.05 eV, a S 1*s* binding energy difference of no more than 0.1 eV would be expected, as typically a S 1*s* binding energy shift is ~1.2 × the corresponding S 2*p* shift (Sodhi and Cavell 1986; Chassé et al. 1993). This was confirmed by the experimentally determined S 1*s* binding energy for α-NiS being 0.1 eV lower than the value for β-NiS.

Near-edge X-ray absorption fine structure spectra

In light of the very similar core electron binding energies observed for α-NiS and β-NiS, detailed comparison of

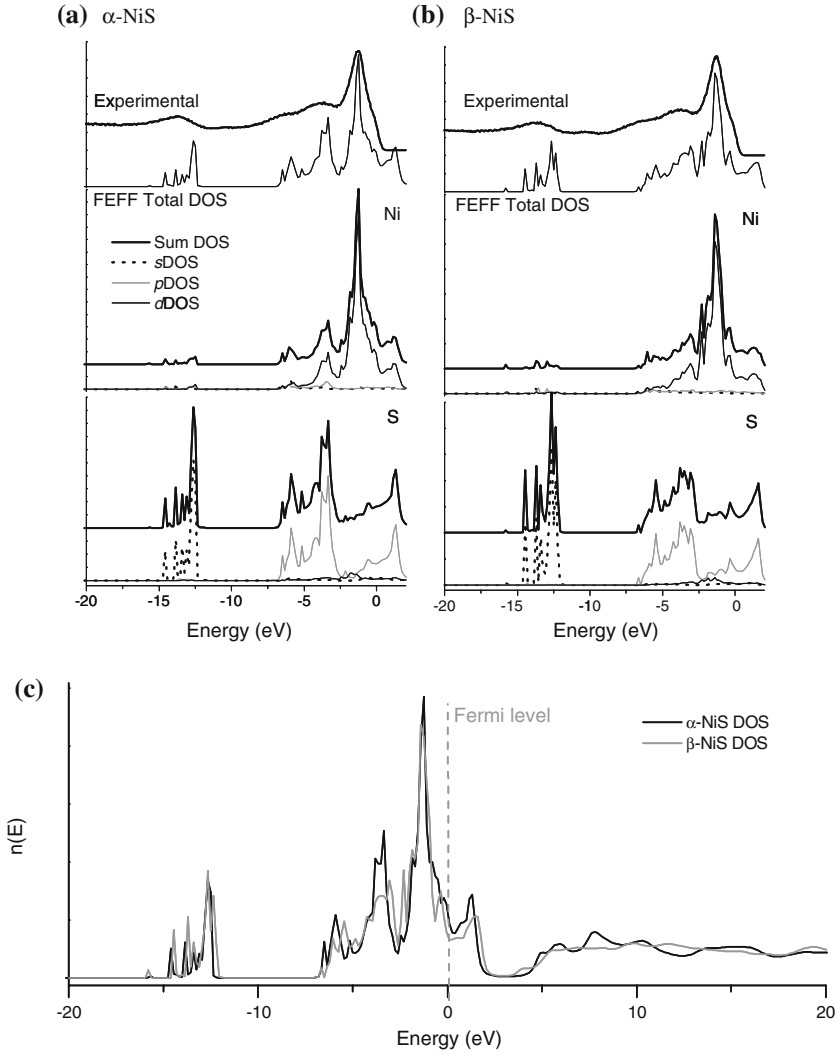

Fig. 3 Comparison of experimental valence photoelectron spectra with FEFF-calculated DOS for **a** α-NiS and **b** β-NiS, and the respective partial densities of occupied states (*s*-, *p*, and *d*-DOS), with each calculated DOS aligned with the Ni *d*-peak in the experimentally obtained valence spectrum; **c** comparison of density of states calculated by FEFF8 for α-NiS with that for β-NiS

the NEXAFS spectra for the two sulfides was of particular interest. Any difference in the NEXAFS spectra would arise from a difference in the two densities of unfilled states. Furthermore, NEXAFS spectra, especially those determined in TFY mode, provide information more representative of the bulk than conventional photoelectron spectra and hence essentially uninfluenced by any surface reconstruction. The S K-edge spectra for α-NiS and β-NiS had been determined by Ovsyannikova (1961), and although these spectra were of limited range and resolution, they appeared to indicate that the initial absorption peak, which would arise from transitions of S 1*s* electrons to unfilled states of predominantly Ni 3*d* and S 3*p* character, was significantly less intense for α-NiS than for β-NiS relative to the intensity of the second, broader absorption peak. The spectra also indicated that the initial peak for α-NiS was at a *lower* energy than that for millerite. In the S K-edge spectrum for hexagonal NiS reported by Sugiura et al. (1974), the absorption maximum of the first peak was obviously greater than that of the second, and at an energy ~3 eV below that for elemental sulfur. The S K-edge absorption spectrum for $Ni_{0.923}S$ reported by Farrell et al. (2000) resembled the spectrum for α-NiS obtained by Ovsyannikova (1961) insofar as the absorption maximum of the first peak was only marginally greater than that of the second. The S K-edge spectrum for finely powdered hexagonal NiS obtained by Zajdel et al. (1999) appeared to be dominated by a contribution from sulfate (Farrell and Fleet 2001), nevertheless for the unoxidized sulfide contribution, the absorption maximum of the first peak was clearly greater than that of the second.

The TEY S K-edge spectra for α-NiS and β-NiS obtained here are shown in Fig. 4. The spectra obtained in TFY mode were similar. It can be seen that the absorption edges are at essentially the same energy, and the relative intensity of the first absorption peaks is very similar (but markedly greater than that of the second peak). The S K-edge spectra simulated by FEFF8 calculations carried out with an unscreened core hole are shown in Fig. 5. The similarity of the two S K-edge spectra is in agreement with the similarity of the calculated densities of unfilled states for α-NiS and β-NiS. The corresponding S 1*s* and 2*p* binding energies calculated by FEFF differed by 0.1 eV only. The densities of unfilled states calculated by means of WIEN2k (which is based on density functional theory) were in good agreement with those obtained using FEFF8. The S K-edge spectrum simulated by Zajdel et al. (1999) for α-NiS using linear muffin tin orbital calculations was similar to the experimental spectra shown in Fig. 4.

As expected from the similar S 2*p* binding energies and calculated densities of unfilled states, the S L-edge NEXAFS spectra for α-NiS and β-NiS were almost identical. The first part (only) of each S $L_{2,3}$-edge spectrum is shown in Fig. 6 to clearly illustrate the almost identical L_3-edge initial peak position for both materials. Again, as expected from the similar Ni 2*p* binding energies and densities of unfilled states, the Ni L-edge spectra too were quite similar (Fig. 7). Relative to the L_3-edge energy for Ni metal of 852.7 eV, the Ni L_3-edge energies for α-NiS and β-NiS were 853.2 and 853.4 eV, respectively.

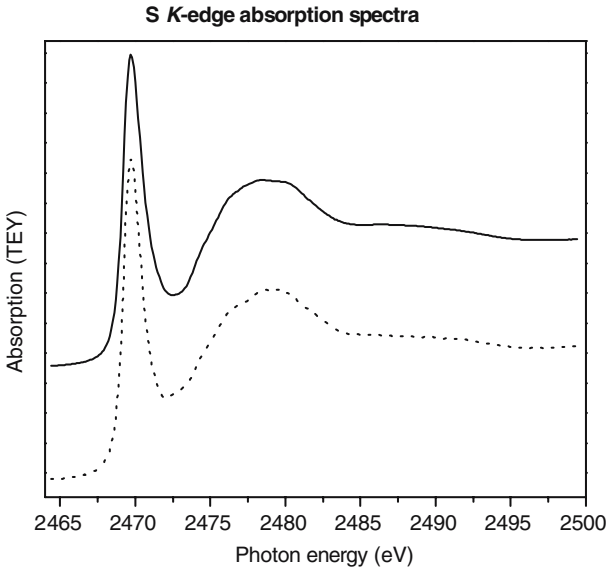

Fig. 4 Sulfur K-edge TEY NEXAFS spectra of α-NiS (*solid line*) and β-NiS (*broken line*)

Discussion

The almost negligible difference in the measured and calculated core electron binding energies for α-NiS and β-NiS does not support the proposition that the S core electron binding energies necessarily increase measurably with coordination number. Indeed, the observed S core electron binding energies are marginally *lower* for hexagonal NiS, not moderately *higher* as might be expected if a general relationship between binding energy and coordination were valid. The S core electron binding energies calculated by FEFF8 also indicated values slightly (~0.1 eV) lower for α-NiS than for β-NiS.

It could be argued that one reason the S core electron binding energies in α-NiS are not significantly different from those in β-NiS is that the metal-sulfur bond in the former is only 6% longer than the shorter bond length in the latter (see Table 1). By contrast, the bond length for 5-coordinate sulfur is up to 14% greater than the 4-coordinate sulfur in pentlandite, and the 6-coordinate Fe–S distance is up to 15% greater than the 5-coordinate in pyrrhotite. Against such an argument, while there is no difference in the bond lengths for the 5-coordinate S in millerite and pentlandite, there is a ~0.5 eV S 2*p* binding energy difference. Although in the latter case both Fe and Ni atoms are involved, the S $2p_{3/2}$ binding energies for 5-coordinate S in NiS (161.7 eV) and Fe_7S_8 (161.25 eV) are both significantly lower than the value for the 5-coordinate S in pentlandite (162.2 eV).

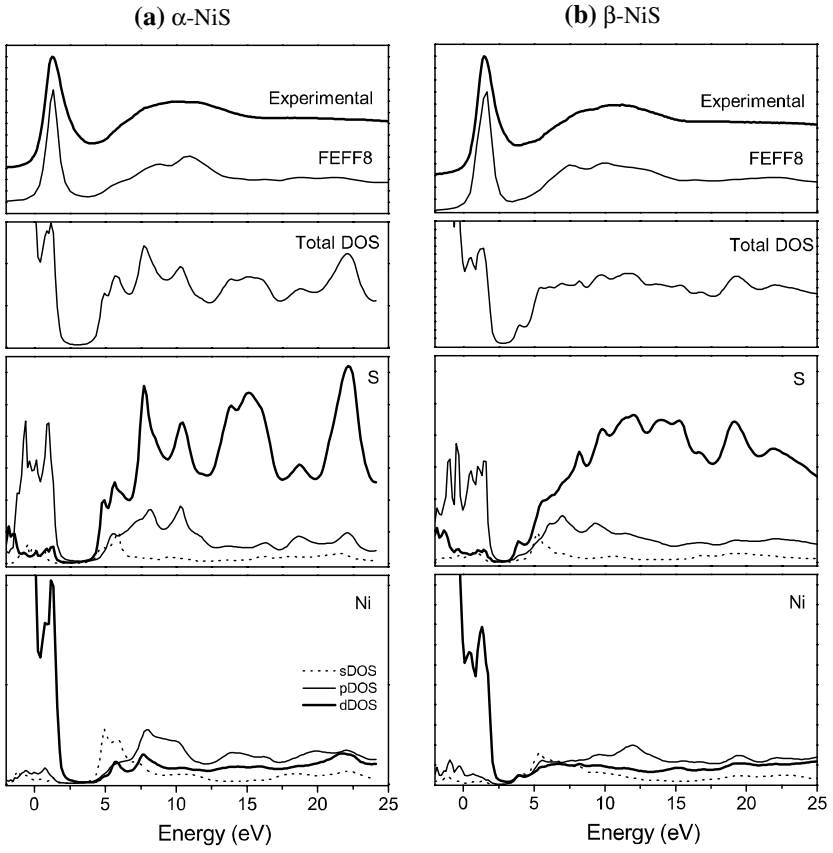

Fig. 5 Comparison of experimental S K-edge NEXAFS spectra for **a** α-NiS and **b** *β*-NiS with theoretical NEXAFS spectra calculated with no core hole and the respective partial densities of unoccupied states (*s*-, *p*-, and *d*-DOS)

There appears to be no convincing evidence to support the possibility that the observed similarity in the spectra for α-NiS and *β*-NiS arose because the surface layer of the metastable α-NiS examined in each case had largely restructured to the rhombohedral phase. Surfaces examined by XPS were prepared immediately before insertion into the spectrometer, and S 2*p* binding energies obtained from gently abraded and fracture surfaces of α-NiS were essentially the same. Surfaces characterized by NEXAFS spectroscopy were also pre-

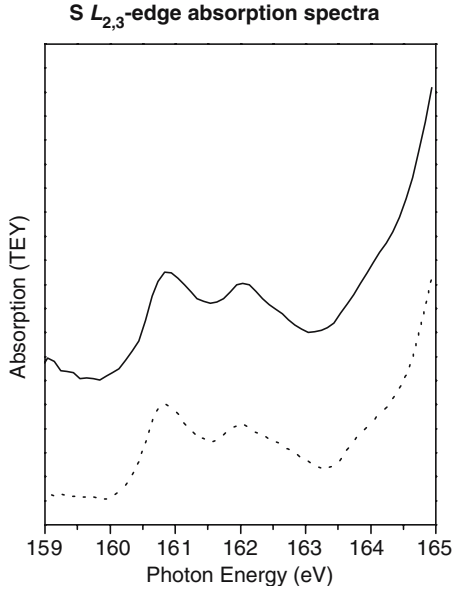

Fig. 6 Low energy region of sulfur $L_{2,3}$-edge TEY NEXAFS spectra of α-NiS (*solid line*) and *β*-NiS (*broken line*)

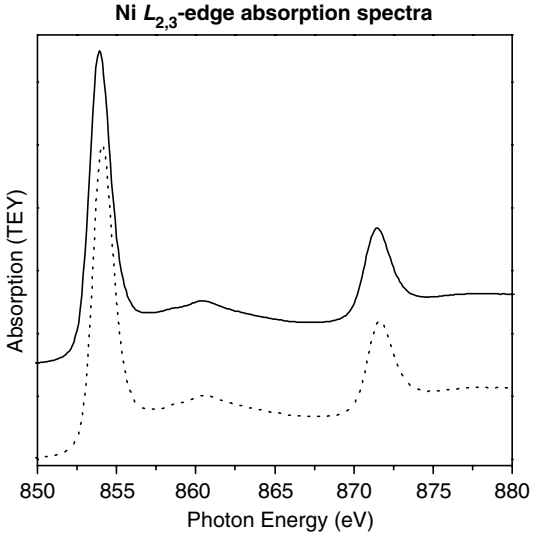

Fig. 7 Nickel $L_{2,3}$-edge TEY NEXAFS spectra of α-NiS (*solid line*) and *β*-NiS (*broken line*)

Table 1 Experimental S 2*p* binding energies and metal–sulfur bond lengths for S atoms with different coordination in relevant Ni and Fe sulfides

Sulfide	Sulfur coordination	S $2p_{3/2}$ binding energy (eV)	Metal–S bond length range (nm)
α-NiS	6	161.65	0.239[f]
β-NiS	5	161.7[a]	0.226–0.238[g]
$(Ni,Fe)_9S_8$	4	161.4[b]	0.215[h]
$(Ni,Fe)_9S_8$	5	162.2[b]	0.226–0.238[h]
Ni_2FeS_4	4	[c]	0.222–0.226[i]
Fe_7S_8	5	161.25[d]	0.232–0.249[j]
Fe_7S_8	6	162.15[d]	0.252–0.267[j]
FeS	6	161.85[e]	0.236–0.272[k]

[a]Legrand et al. (1998) and present study
[b]Legrand et al. (1997)
[c]Binding energy reported to be the same as for pentlandite (Richardson and Vaughan 1989)
[d]Nesbitt et al. (2001)
[e]Skinner et al. (2004)
[f]Trahan et al. (1970)
[g]Rajamani and Prewitt (1974)
[h]Rajamani and Prewitt (1973)
[I]Charnock et al. (1990)
[j]Tokonami et al. (1972)
[k]Keller-Besrest and Collin (1990)

pared immediately before insertion into the end-station, and the analysis depth for TEY mode at the S K-edge is greater than for the XPS measurements. Spectra obtained in TFY mode, for which the analysis depth is considerably larger than for TEY, were similar to those obtained in TEY mode. A small but reproducible difference in the S 2*p* binding energies for the two structural forms was observed. Furthermore, the subtle but reproducible differences in the valence band spectra were consistent with the densities of states calculated by both FEFF8 and WIEN2k.

Even if a general relationship between binding energy and coordination number for a particular metal in different sulfide structural environments is not valid, it does not necessarily mean that the proposed 2*p* binding energies for 5-coordinate and 6-coordinate S in pyrrhotite (Nesbitt et al. 2001), or 4-coordinate and 5-coordinate S in pentlandite (Legrand et al. 1997, 2005), are not correct. However, in the case of pyrrhotite, FEFF8-calculated core electron binding energies which are larger for the 5-coordinate S than for the 6-coordinate S might be considered sufficient reason to re-examine the interpretation of the experimental spectra. In the case of pentlandite, at least one of the alternative assignments considered previously should definitely be re-assessed (Legrand et al. 1997; Buckley and Woods 1991b). Other evidence, including NEXAFS measurements and FEFF8 simulations for pentlandite (Goh et al. 2005, unpublished data), suggests that in pentlandite, the 4-coordinate S has a 2*p* binding energy considerably less than 0.8 eV below that for the 5-coordinate S, which would be inconsistent with the interpretation of Legrand et al. (1997, 2005). Hence the hypothesis that the loss of one coordinating cation causes a negative S 2*p* binding energy shift of about 0.8 eV should be reassessed.

Conclusion

The photoelectron spectra for α-NiS and β-NiS were found to be similar, although subtle differences in electronic environment were more evident in the NEXAFS spectra. The measured and calculated core electron binding energies did not support the previously postulated relationship between S coordination number and electron binding energies for the same metal in different sulfide environments. However, that does not necessarily invalidate assignments of S 2*p* spectra for pentlandite and pyrrhotite proposed previously on the basis of this general relationship. Nevertheless, there is now sufficient evidence to suggest that an alternative assignment for pentlandite in particular should be re-evaluated.

Acknowledgements This work was supported by the Australian Synchrotron Research Program, which is funded by the Commonwealth of Australia under the Major National Research Facilities Program. The authors are grateful to Dr Damian Moran, University of Sydney, for assistance in carrying out large-cluster FEFF8 calculations on a supercomputer available through the Australian Partnership for Advanced Computing National Facility, and to Dr Vicki J. Keast, University of Sydney, for advice on using WIEN2k. Dr Craig Klauber, CSIRO Minerals, kindly provided the millerite specimen used in the investigation.

References

Ankudinov AL, Bouldin CE, Rehr JJ, Sims J, Hung H (2002) Parallel calculation of electron multiple scattering using Lanczos algorithms. Phys Rev B 65:104107-1–104107-11

Ankudinov AL, Ravel B, Rehr JJ, Conradson SD (1998) Real-space multiple-scattering calculation and interpretation of x-ray-absorption near-edge structure. Phys Rev B 58:7565–7576

Bagus PS, Illas F, Pacchioni G, Parmigiani F (1999) Mechanisms responsible for chemical shifts of core-level binding energies and their relationship to chemical bonding. J Electron Spectrosc 100:215–236

Buckley AN, Woods R (1984) An X-ray photoelectron spectroscopic study of the oxidation of galena. Appl Surf Sci 17:401–414

Buckley AN, Woods R (1991a) Electrochemical and XPS studies of the surface oxidation of synthetic heazlewoodite (Ni_3S_2). J Appl Electrochem 21:575–582

Buckley AN, Woods R (1991b) Surface composition of pentlandite under flotation-related conditions. Surf Interface Anal 17:675–680

Charnock J, Garner CD, Pattrick RAD, Vaughan DJ (1990) An EXAFS study of thiospinel minerals. Am Mineral 75:247–255

Chassé T, Peisert H, Streubel P, Szargan R, Meisel A (1993) XPS binding energies of deep core levels and the Auger parameter—an application to solid sulfur compounds. Acta Phys Polonica A 83:793–802

Citrin PH (1973) High-resolution X-ray photoemission from sodium metal and its hydroxide. Phys Rev B 8:5545–5556

Clifford RK, Purdy KL, Miller JD (1975) Characterization of sulfide mineral surfaces in froth flotation systems using electron spectroscopy for chemical analysis. AIChE Symp Ser 71:138–147

Doniach S, Sunjic M (1970) Many-electron singularity in X-ray photoemission and X-ray line spectra from metals. J Phys C Solid State Phys 3:285–291

Egelhoff WF Jr (1987) Core-level binding-energy shifts at surfaces and in solids. Surf Sci Rep 6:253–415

Farrell SP, Fleet ME (2001) Sulfur K-edge XANES study of local electronic structure in ternary monosulfide solid solution [(Fe, Co, Ni)$_{0.923}$S]. Phys Chem Minerals 28:17–27

Farrell SP, Fleet ME, Liu X (2000) XANES spectroscopy of metal sulfides: S K edge of monosulfide solid solution [(Fe,Co,-Ni)$_{0.923}$S] and niningerite [(Mg,Fe,Mn)S], and Ti L edge of Ti sulfides. In: Proceedings of GeoCanada 2000—The Millenium Geoscience Summit Conference, Calgary, Canada, pp 276–279

Grice JD, Ferguson RB (1974) Crystal structure refinement of millerite (β-NiS). Can Mineral 12:248–252

Hunter BA (1998) Rietica—a visual Rietveld program. Comm Powder Diffraction Newsl 20:21–23

Keller-Besrest F, Collin G (1990) Structural aspects of the α transition in stoichiometric FeS: identification of the high-temperature phase. J Solid State Chem 84:194–210

Kravtsova AN, Stekhin IE, Soldatov AV, Fleet ME, Harmer SL (2005) Local and electronic structure of FeS, CoS, NiS: ultrasoft sulfur $L_{2,3}$ X-ray absorption spectra analysis. J Electron Spectrosc 144–147:525–527

Krishnakumar SR, Shanthi N, Priya Mahadevan, Sarma DD (2000) Electronic structure of $NiS_{1-x}Se_x$. Phys Rev B 61:16370–16376. Erratum. Phys Rev B 62:10570–10571

Krishnakumar SR, Shanthi N, Sarma DD (2002) Electronic structure of millerite NiS. Phys Rev B 66:115105

Legrand DL, Bancroft GM, Nesbitt HW (1997) Surface characterization of pentlandite, $(Fe,Ni)_9S_8$, by X-ray photoelectron spectroscopy. Int J Miner Process 51:217–228

Legrand DL, Nesbitt HW, Bancroft GM (1998) X-ray photoelectron spectroscopic study of a pristine millerite (NiS) surface and the effect of air and water oxidation. Am Mineral 83:1256–1265

Legrand DL, Bancroft GM, Nesbitt HW (2005) Oxidation/alteration of pentlandite and pyrrhotite surfaces at pH 9.3: Part 1. Assignment of XPS spectra and chemical trends. Am Mineral 90:1042–1054

Mårtensson N, Nilsson A (1995) On the origin of core-level binding energy shifts. J Electron Spectrosc 75:209–223

McWhan DB, Marezio M, Remeika JP, Dernier PD (1972) Pressure–temperature phase diagram and crystal structure of NiS. Phys Rev B 5:2552–2555

Nesbitt HW, Schaufuss AG, Scaini M, Bancroft GM, Szargan R (2001) XPS measurement of fivefold and sixfold coordinated sulfur in pyrrhotites and evidence for millerite and pyrrhotite surface species. Am Mineral 86:318–326

Ovsyannikova IA (1961) The X-ray spectrum of nickel sulfides. Izv Sibirsk Otd Akad Nauk SSSR pp 80–87

Rajamani V, Prewitt CT (1973) Crystal chemistry of natural pentlandites. Can Mineral 12:178–187

Rajamani V, Prewitt CT (1974) The crystal structure of millerite. Can Mineral 12:253–257

Ravel B (2001) *ATOMS*: crystallography for the X-ray absorption spectroscopist. J Synchrotron Rad 8:314–316

Ravel B (2004) FEFF Users http://www.cars9.uchicago.edu/feff/feffusers/msg00212.html

Raybaud P, Hafner J, Kresse G, Toulhoat H (1997) *Ab initio* density functional studies of transition-metal sulphides: II. Electronic structure. J Phys Condens Matter 9:11107–11140

Schaufuß AG, Nesbitt HW, Kartio I, Laajalehto K, Bancroft GM, Szargan R (1998) Incipient oxidation of fractured pyrite surfaces in air. J Electron Spectrosc 96:69–82

Richardson S, Vaughan DJ (1989) Surface alteration of pentlandite and spectroscopic evidence for secondary violarite formation. Miner Mag 53:213–222

Šimůnek A, Vackář J, Kunc K (2005) Core energy levels of Sc and N and their variation with coordination number in ScN. Phys Rev B 72:045110-1–045110-4

Skinner WM, Nesbitt HW, Pratt AR (2004) XPS identification of bulk hole defects and itinerant Fe 3d electrons in natural troilite (FeS). Geochim Cosmochim Acta 68:2259–2263

Sodhi RNS, Cavell RG (1986) *KLL* Auger and core level (1*s* and 2*p*) photoelectron shifts in a series of gaseous sulfur compounds. J Electron Spectrosc 41:1–24

Sugiura C, Gohshi Y, Suzuki I (1974) Sulfur $K\ \beta$ x-ray emission spectra and electronic structures of some metal sulfides. Phys Rev B 10:338–343

Thomas JE, Skinner WM, Smart RStC (2003) A comparison of the dissolution behaviour of troilite with other iron(II) sulfides; implications of structure. Geochim Cosmochim Acta 67:831–843

Tokonami M, Nishiguchi K, Morimoto N (1972) Crystal structure of a monoclinic pyrrhotite (Fe_7S_8). Am Mineral 57:1066–1080

Trahan J, Goodrich RG, Watkins SF (1970) X-ray diffraction measurements on metallic and semiconducting hexagonal NiS. Phys Rev B 2:2859–2863

Usuda M, Hamada N (2000) Empirical LSDA + U study for electronic structure of hexagonal NiS. J Phys Soc Jpn 69:744–748

Vaughan DJ, Craig JR (1985) The crystal chemistry of iron-nickel thiospinels. Am Mineral 70:1036–1043

Wang H, Pring A, Ngothai Y, O'Neill B (2006) The kinetics of the $\alpha \rightarrow \beta$ transition in synthetic nickel monosulfide. Am Mineral 91 (in press)

Zajdel P, Kisiel A, Zimnal-Starnawska M, Lee PM, Boscherini F, Giriat W (1999) XANES study of sulphur K edges of transition metal (V, Cr, Mn, Fe, Co, Ni) monosulphides: experiment and LMTO numerical calculations. J Alloys Compounds 286:66–70